Supporting information

Broad-Spectrum Ultrathin-Metal-Based Oxide/Metal/Oxide Transparent Conductive Films for Optoelectronic Devices

Zhang Liu[+,1], Yalu Zou[+,2], Chengang Ji[+,3], Xinliang Chen[*,1], Guofu Hou [1], Cong Zhang [1], Xiangjian Wan [2], L. Jay Guo [3], Ying Zhao [1], Xiaodan Zhang [1]*

[1] Institute of Photo-electronic Thin Film Devices and Technology, Key Laboratory of Photo-electronic Thin Film Devices and Technology of Tianjin, College of Electronic Information and Optical Engineering, Nankai University, Tianjin 300350, China

[2] Key Laboratory of Functional Polymer Materials, Renewable Energy Conversion and Storage Center (RECAST), College of Chemistry, Nankai University, Tianjin 300071, China

[3] Department of Electrical Engineering and Computer Science, University of Michigan, Ann Arbor, Michigan 48109, United States

Keywords: broad-spectrum, transparent conductive films, ultrathin metal film, oxide/metal/oxide, optoelectronic devices

---

[+] *Z. Liu, Y.L. Zou, C.G. Ji contributed equally to this work.*

[*]*Corresponding Author. E-mail: cxlruzhou@163.com (X.L. Chen)*

I. Comparison of the properties of Ag-Zn thin films on different substrates (including the optical, electrical and structural performances).

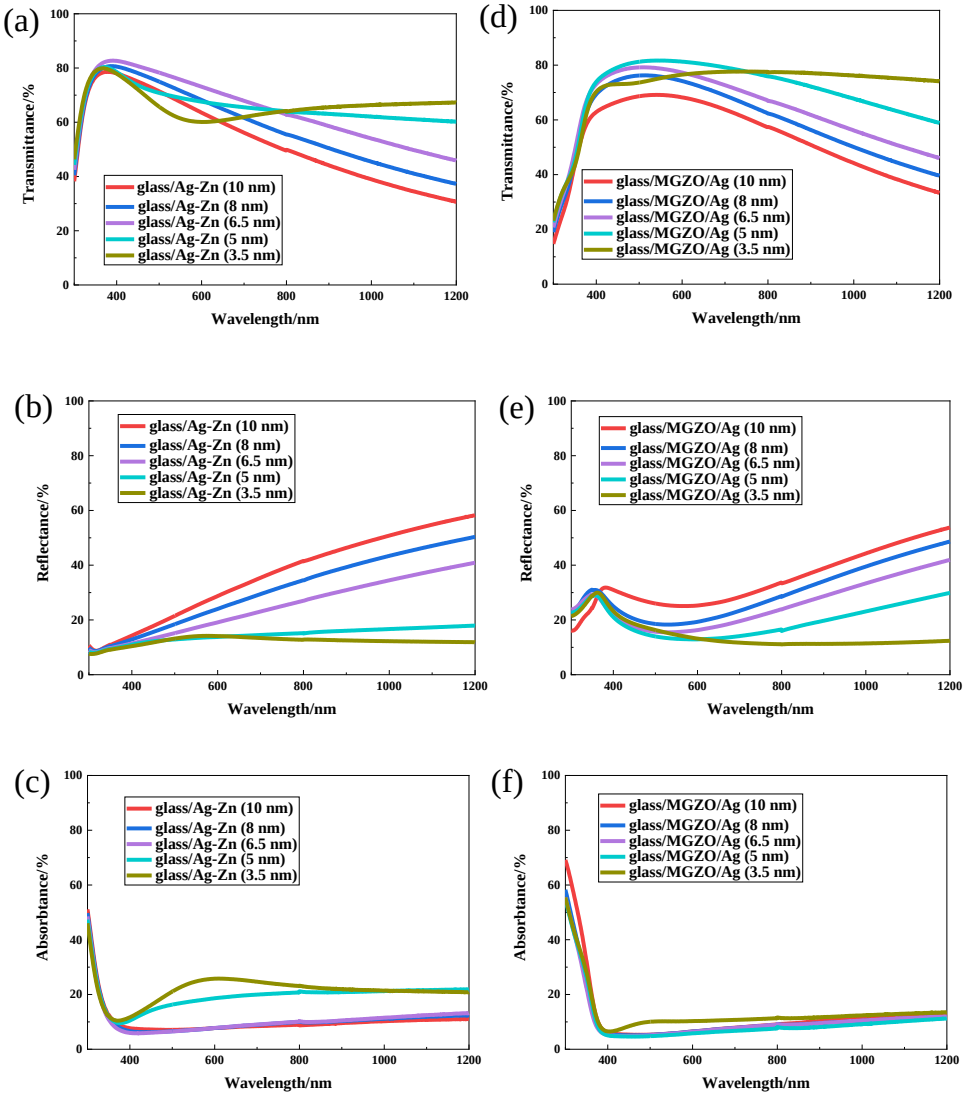

Figure S1. (a) Transmittance, (b) reflectance, (c) absorbance of glass/Ag-Zn thin films, and (d) transmittance, (e) reflectance, (f) absorbance of glass/MGZOAg-Zn thin films with different thickness of Ag-Zn films. It can be observed that the turning point of transmittance and absorbance is 6.5 nm on glass substrate and 5 nm on glass/MGZO substrate, respectively.

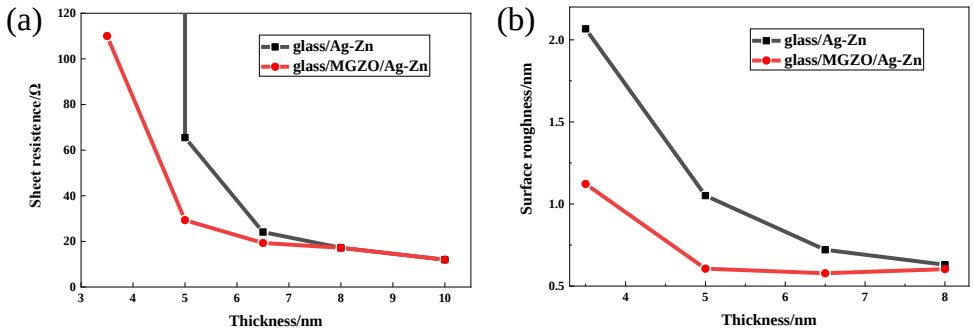

Figure S2. (a) Sheet resistance and (b) surface roughness of glass/Ag-Zn and glass/MGZO/Ag-Zn with different thicknesses of Ag-Zn films. The falling speed of sheet resistance and surface roughness of Ag-Zn films on glass/MGZO substrate is significantly faster than that on glass substrate, which indicates MGZO can promote the nucleation of Ag-Zn thin films.

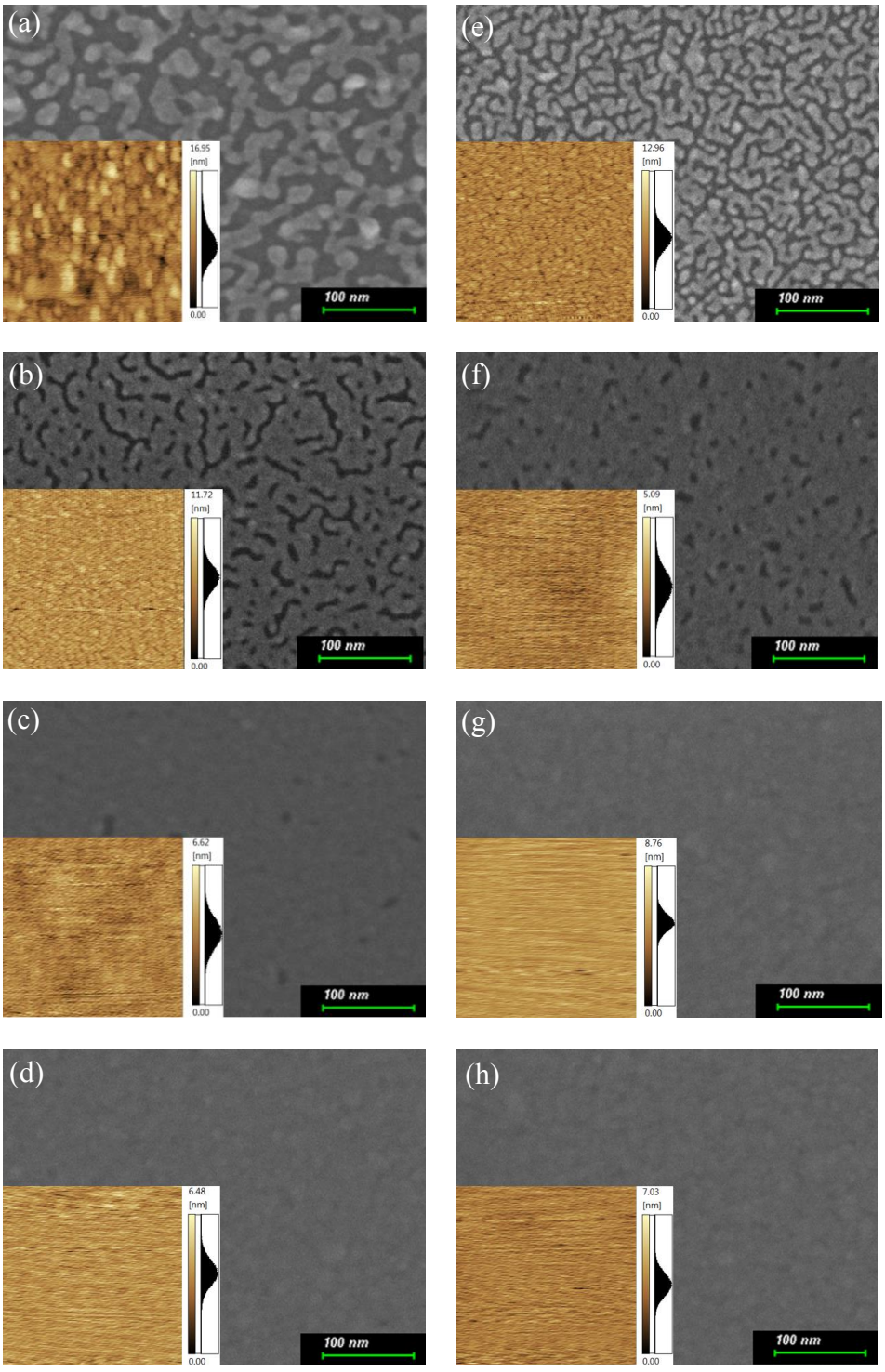

Figure S3. The surface morphology of glass/Ag-Zn with different thicknesses of Ag-Zn films: (a) 3.5 nm; (b) 5 nm; (c) 6.5 nm; (d) 8 nm; The surface morphology of glass/MGZO/Ag-Zn with different thickness of Ag-Zn films: (e) 3.5 nm; (f) 5 nm; (g) 6.5 nm; (h) 8 nm (The scanning range of AFM is 500 × 500 nm^2). The thickness of the Ag-Zn film continuously formed on the glass substrate and the glass/MGZO substrate (the threshold thickness) is 6.5 nm and 5 nm, respectively.

II. Optical, electrical and structural performances of Ag-Al thin films.

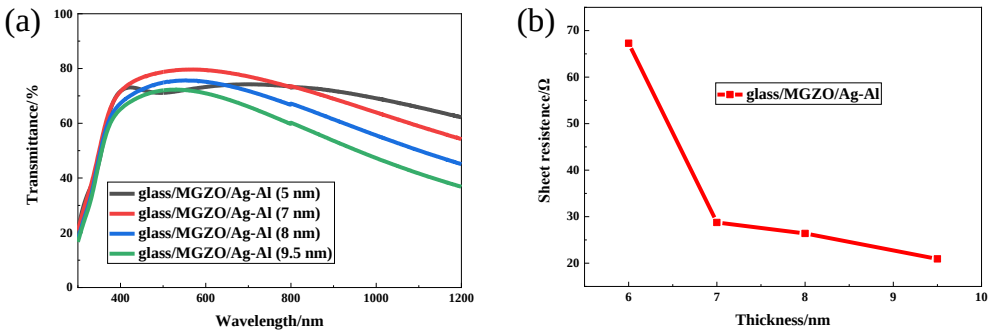

Figure S4. (a) Transmittance and (b) sheet resistance of glass/MGZO/Ag-Al with different thicknesses of Ag-Al films. According to the turning point of transmittance and the sudden increase point of sheet resistance, it can be considered that the threshold thickness of Ag-Al thin film is 7 nm on the glass/MGZO substrate.

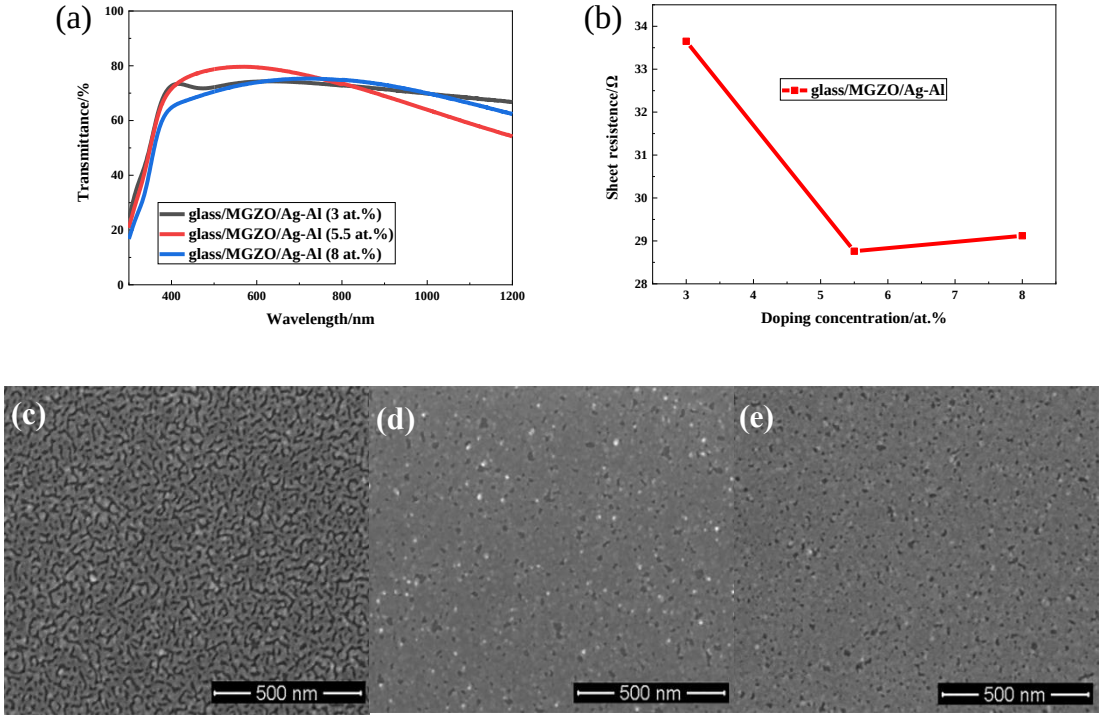

Figure S5. (a) Transmittance and (b) sheet resistance of glass/MGZO/7 nm Ag-Al films with different doping concentrations; SEM image of glass/MGZO/7 nm Ag-Al films with different doping concentrations: (c) 3 at.%; (d) 5.5 at.%; (e) 8 at.%. Considering the optical performance, electrical performance and surface morphology, 5.5 at.% is considered as the optimized Al doping concentration.

III. Effect of different oxygen flow rate on performance of 4 nm thick Ag-Zn(O) thin films.

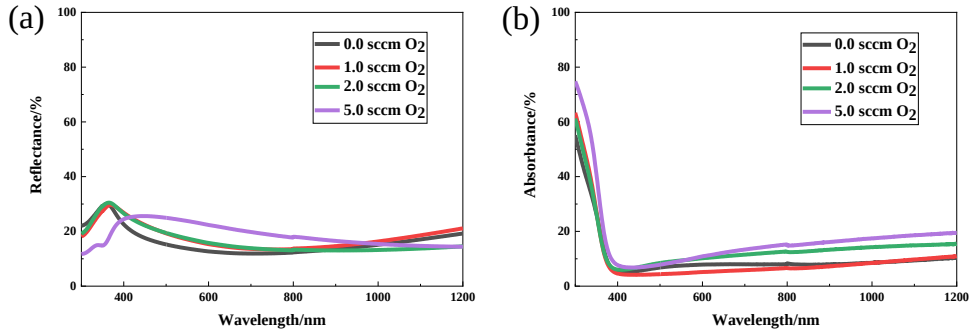

Figure S6. (a) Reflectance and (b) absorbance of glass/MGZO/Ag-Zn(O) films with different O_2 flow. The reflectance increases with the increase of oxygen flow. The average absorbance has decreased from 8% to 6.8% (λ~400-1200 nm), when 1.0 sccm O_2 is introduced.

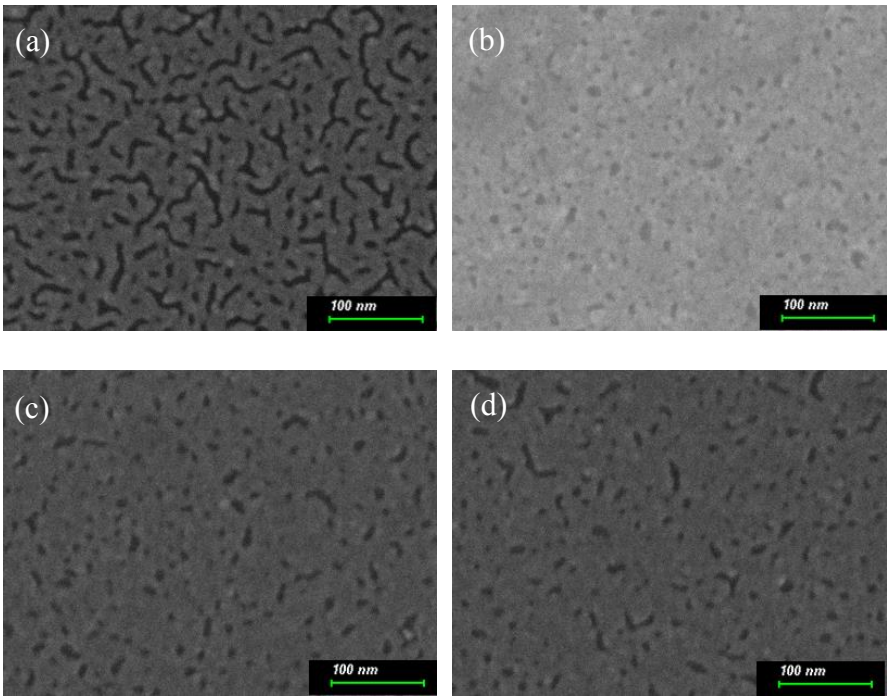

Figure S7. The surface morphology of glass/MGZO/Ag-Zn(O) with different O_2 flow rates: (a) 0 sccm; (b) 1.0 sccm; (c) 2.0 sccm; (d) 5.0 sccm. The 4 nm thick Ag-Zn(O) film transforms from a surface morphology with lots of unfilled gaps to a continuous surface.

IV. Optical and electrical influences of trace O_2 on the threshold thickness of Ag-Zn(O) thin films.

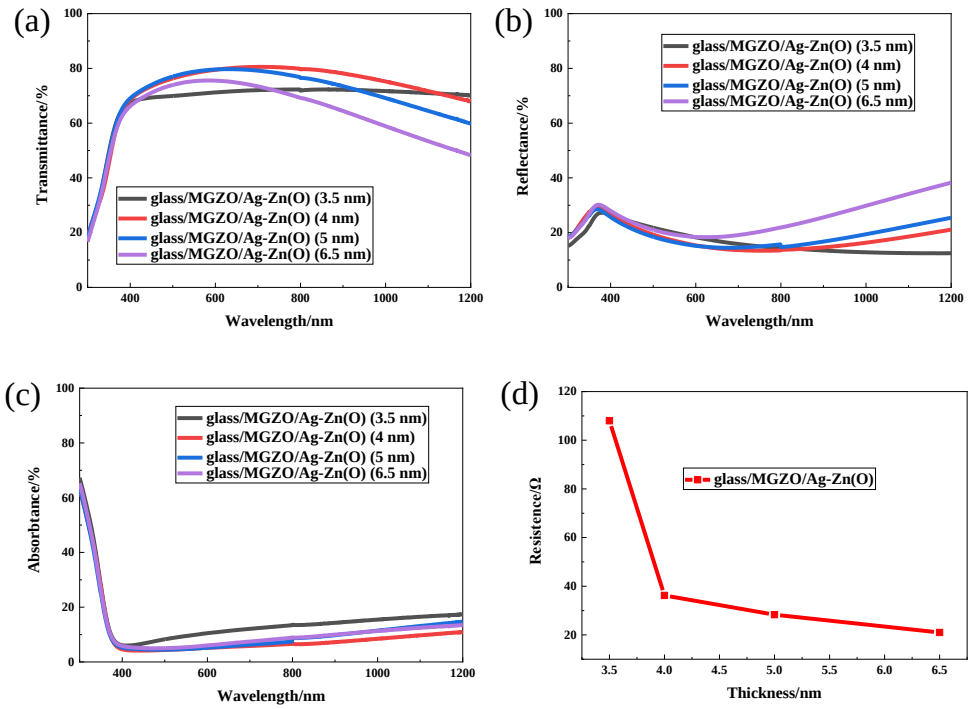

Figure S8. (a) Transmittance, (b) reflectance, (c) absorbance, (d) sheet resistance of glass/MGZO/Ag-Zn(O) with different thickness of Ag-Zn(O) films (The O_2 flow is fixed at 1.0 sccm).

V. Optical, electrical and structural performances of Ag-CdO thin films.

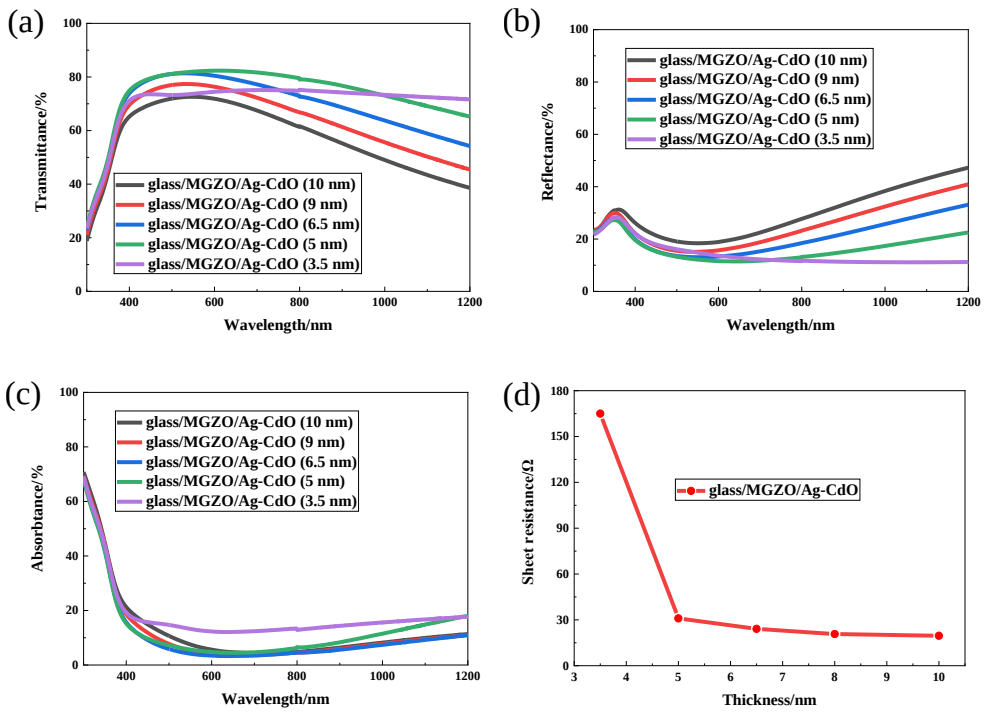

Figure S9. (a) transmittance, (b) reflectance, (c) absorbance and (d) sheet resistance of glass/MGZO/Ag-CdO with different thicknesses of Ag-CdO films.

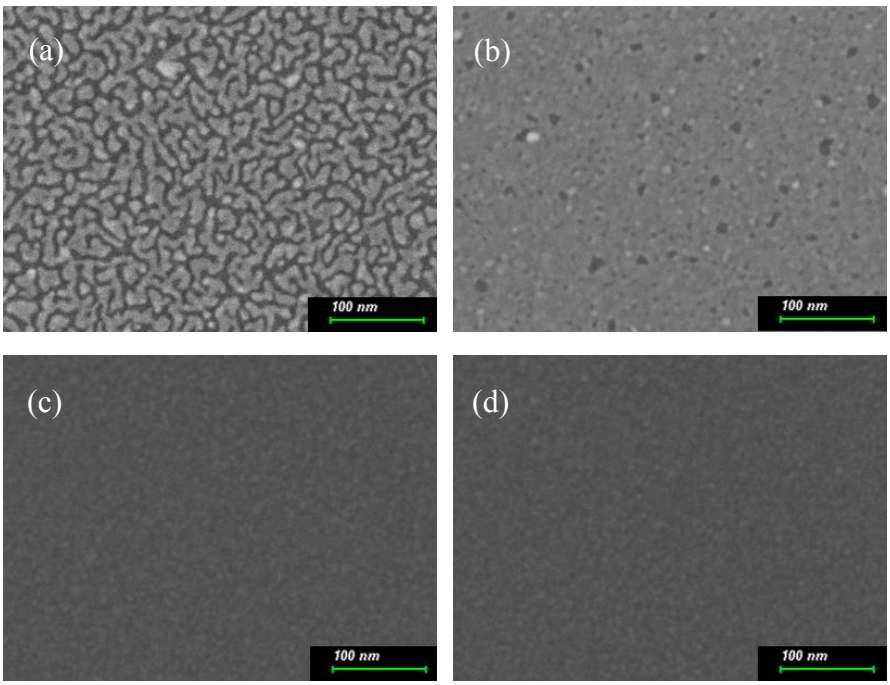

Figure S10. The surface morphology of glass/MGZO/Ag-CdO with different thicknesses of Ag-CdO films: (a) 3.5 nm; (b) 5 nm; (c) 6.5 nm; (d) 8 nm.

VI. Performances of organic solar cells (OSCs) based on commercialized glass/ITO and glass/OMO (MGZO/Ag/MGZO) electrodes.

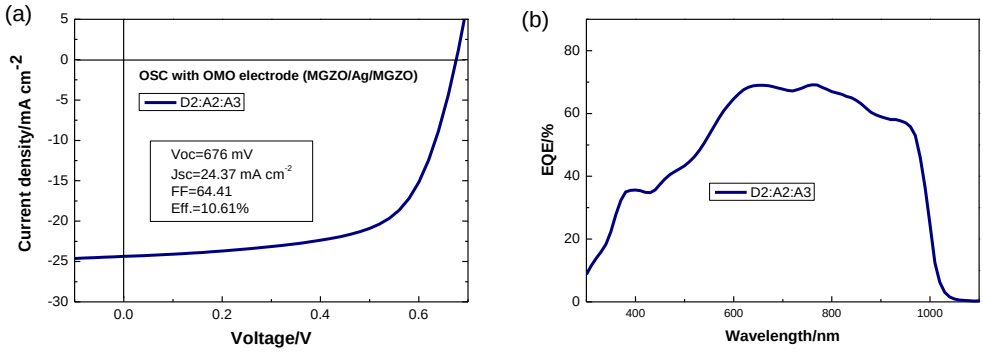

Figure S11. (a) *J-V* curve and (b) EQE spectrum of OSC based on glass/OMO (MGZO/Ag/MGZO) electrode with the photoactive layer of D2:A2:A3.

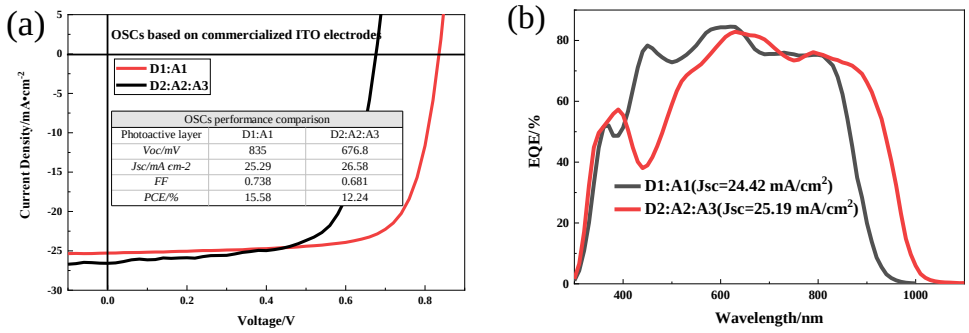

Figure S12. (a) *J-V* characteristics and (b) EQE spectra of OSCs based on commercialized glass/ITO electrodes with different photoactive layers.

VII. Table summary of typical OMO (oxide-metal-oxide) thin films.

Table S1. Summary of optical and electrical properties of typical OMO compound films.

OMO structure (nm)	Transmittance	Sheet resistance (Ω/sq)	Reference
Ag-Al/ZnO (7/40)	92% (550 nm) ＞80% (400-800 nm)	23.4	[1]
ITO/Ag-Cu/ITO (40/8/40)	98.5% (600 nm) ＞96% (400-700 nm)	12.6	[2]
ZnO/Ag-Cu/Al_2O_3 (24 /6.5 /56)	100.3% (400-700)	18.6	[3]
AZO/Ag-SnO_x/AZO (40/6/40)	79.1% (550 nm)	10.8	[4]
Al_2O_3/Ag/MoO_x (40 /9 /20)	93.85% (550 nm)	7.39	[5]
ZnO/MUA/Ag/ZnO (40/*/10/20)	＞80% (400-600 nm)	8.61	[6]
ZnO/Cu(N)/ZnO (60/6.5/60)	84% (380-1000 nm)	20	[7]
MoO_3/Au/MoO_3 (30/7/80)	~80% (500-700 nm) 74% (800-1100 nm)	19.6	[8]
ZnO/AgO_x/ZnO (50/6/50)	92% (400-1000 nm)	26.5	[9]
AZO/Ag/AZO (35/6/30)	93.6 (500 nm)	5.6	[10]
SnO_x/Ag/SnO_x (20/7/20)	81% (390-780 nm)	10	[11]
MGZO/Ag/MGZO (40/9.5/45)	94.7% (400-800 nm)	10	[12]
ZnO/AgO_x/Ag/ZnO (5/1.5/6/25)	94% (400-800 nm)	12.5	[13]

Table S2. Lattice strains and crystallite sizes of the 100-nm thick Ag-Zn(O) film with different O_2 flow rates determined from the Ag (111) peak.

O_2 flow rate/sccm	Peak position/2θ	FWHM/2θ	Lattice strain/%	Crystallite size/nm
0	38.26	0.64	0.81	12.0
1.0	38.06	0.81	1.02	10.2
2.0	38.12	1.05	1.32	7.9
5.0	38.16	1.56	1.97	5.3

References

(1) Zhang, C.; Zhao, D.; Gu, D.; Kim, H.; Ling, T.; Wu, Y. K.; Guo, L. J. An Ultrathin, Smooth, and Low-loss Al-doped Ag Film and Its Application as a Transparent Electrode in Organic Photovoltaics. *Adv. Mater.* **2014,** *26* (32), 5696-5701.

(2) Wang, H.; Ji, C.; Zhang, C.; Zhang, Y.; Zhang, Z.; Lu, Z.; Tan, J.; Guo, L. J. Highly Transparent and Broadband Electromagnetic Interference Shielding Based on Ultrathin Doped Ag and Conducting Oxides Hybrid Film Structures. *ACS Appl. Mater. Inter.* **2019,** *11* (12), 11782-11791.

(3) Ji, C.; Liu, D.; Zhang, C.; Jay Guo, L. Ultrathin-Metal-Film-Based Transparent Electrodes with Relative Transmittance Surpassing 100. *Nat. Commun.* **2020,** *11* (1), 3367.

(4) Wang, Z.; Li, J.; Xu, J.; Huang, J.; Yang, Y.; Tan, R.; Chen, G.; Fang, X.; Zhao, Y.; Song, W. Robust Ultrathin and Transparent AZO/Ag-SnO /AZO on Polyimide Substrate for Flexible Thin Film Heater with Temperature Over 400 °C. *J. Mater. Sci. Technol.* **2020,** *48*, 156-162.

(5) Yang, X.; Gao, P.; Yang, Z.; Zhu, J.; Huang, F.; Ye, J. Optimizing Ultrathin Ag Films for High Performance Oxide-Metal-Oxide Flexible Transparent Electrodes through Surface Energy Modulation and Template-stripping Procedures. *Sci. Rep.* **2017,** *7*, 44576.

(6) Zou, J.; Li, C.; Chang, C.; Yip, H.; Jen A. Interfacial Engineering of Ultrathin Metal Film Transparent Electrode for Flexible Organic Photovoltaic Cells. *Adv. Mater.* **2014**, *26*, 3618-3623.

(7) Zhao, G.; Kim, S. M.; Lee, S.-G.; Bae, T.-S.; Mun, C.; Lee, S.; Yu, H.; Lee, G.-H.; Lee, H.-S.; Song, M.; Yun, J. Bendable Solar Cells from Stable, Flexible, and Transparent Conducting Electrodes Fabricated Using a Nitrogen-doped Ultrathin Copper Film. *Adv. Funct. Mater.* **2016,** *26* (23), 4180-4191.

(8) Wang, Z.; Zhu, X.; Zuo, S.; Chen, M.; Zhang, C.; Wang, C.; Ren, X.; Yang, Z.;, Liu, Z.; Xu, X.; Chang, Q.; Yang, S.; Meng, F.; Liu, Z.; Yuan, N.; Ding, J.; Liu, S.; Yang, D. 27%-efficiency Four-terminal Perovskite/silicon Tandem Solar Cells by Sandwiched Gold Nanomesh. *Adv. Funct. Mater.* **2019**, 1908298.

(9) Wang, W.; Song, M.; Bae, T.-S.; Park, Y. H.; Kang, Y.-C.; Lee, S.-G.; Kim, S.-Y.; Kim, D. H.; Lee, S.; Min, G.; Lee, G.-H.; Kang, J.-W.; Yun, J. Transparent Ultrathin Oxygen-doped Silver Electrodes for Flexible Organic Solar Cells. *Adv. Funct. Mater.* **2014,** *24* (11), 1551-1561.

(10) Li, P.; Li, H.; Ma, J.; Zhou, Y.; Zhang, W.; Cong, L.; Xu, H.; Liu, Y. Structural Optimization of Oxide/Metal/Oxide Transparent Conductors for High-performance Low-emissivity Heaters. *Adv. Mater. Inter.* **2018,** *5* (24), 1801287.

(11) Zhao, J.; Brinkmann, K.; Hu, T.; Pourdavoud, N.; Becker, T.; Gahlmann, T.; Heiderhoff, R.; Polywka, A.; Görrn, P.; Chen, Y.; Cheng, B.; Riedl, T. Self-encapsulating Thermostable and Air-resilient Semitransparent Perovskite Solar Cells. *Adv. Energy Mater.* **2017**, *7*, 1602599.

(12) Zhang, Y.; Liu, Z.; Ji, C.; Chen, X.; Hou, G.; Li, Y.; Zhou, X.; Cui, X.; Yang, X.; Ren, C.; Liu, D.; Guo, L. J.; Zhao, Y.; Zhang, X. Low-temperature Oxide/Metal/Oxide Multilayer Films as Highly Transparent Conductive Electrodes for Optoelectronic Devices. *ACS Appl. Energy Mater.* **2021,** 4(7), 6553-6561.

(13) Zhao, G.; Shen, W.; Jeong, E.; Lee, S.G.; Yu, S.M.; Bae, T.S.; Lee, G.H.; Han, S.Z.; Tang, J.; Choi, E.A.; Yun, J. Ultrathin Silver Film Electrodes with Ultralow Optical and Electrical Losses for Flexible Organic Photovoltaics. *ACS Appl. Mater. Inter.* **2018**, *10*, 27510-27520.